

Quantum nondemolition measurements of a qubit coupled to a harmonic oscillator

Luca Chirolli* and Guido Burkard†

RWTH Aachen University, D-52056 Aachen, Germany

and Department of Physics, University of Konstanz, D-78457 Konstanz, Germany

(Received 4 June 2009; revised manuscript received 6 October 2009; published 18 November 2009)

We theoretically describe the weak measurement of a two-level system (qubit) and quantify the degree to which such a qubit measurement has a quantum nondemolition (QND) character. The qubit is coupled to a harmonic oscillator, which undergoes a projective measurement. Information on the qubit state is extracted from the oscillator measurement outcomes, and the QND character of the measurement is inferred from the result of subsequent measurements of the oscillator. We use the positive operator valued measure (POVM) formalism to describe the qubit measurement. Two mechanisms lead to deviations from a perfect QND measurement: (i) the quantum fluctuations of the oscillator, and (ii) quantum tunneling between the qubit states $|0\rangle$ and $|1\rangle$ during measurements. Our theory can be applied to QND measurements performed on superconducting qubits coupled to a circuit oscillator.

DOI: 10.1103/PhysRevB.80.184509

PACS number(s): 03.65.Ta, 03.67.Lx, 42.50.Dv, 42.50.Pq

I. INTRODUCTION

The possibility to perform repeated quantum measurements on a system with the least possible disturbance was first envisioned in the context of measuring gravitational waves.¹ In quantum optics, the optical Kerr effect provided an early playground for studying quantum nondemolition (QND) measurements,^{2–4} that were extended to the framework of cavity quantum electrodynamics (cavity-QED) and mesoscopic mechanical oscillators.^{5–9}

The application of such a scheme to quantum information has stimulated great interest, in particular in the field of quantum computation, where fast and efficient readout is necessary, and error correction plays an important role.¹⁰ Schemes for qubit QND measurements have been theoretically proposed and experimentally realized with a superconducting qubit coupled to harmonic oscillators, either represented by an external tank LC circuit,^{11–17} or by a superconducting resonator that behaves as a one mode quantum harmonic oscillator in circuit-QED.^{18–24} A measurement scheme based on the Josephson bifurcation amplifier (JBA) (Refs. 25 and 26) has been adopted with the aim to perform QND measurements of superconducting qubit.^{27,28} In these experiments a deviation of $\sim 10\%$ from perfect QND behavior has been found.

Motivated by those recent experimental achievements, we analyze a measurement technique based on the coupling of the qubit to a driven harmonic oscillator. A quadrature of the harmonic oscillator is addressed via a projective measurement. The qubit that is coupled to the oscillator affects the outcomes of the measurement of the oscillator and information on the qubit state can be extracted from the results of the projective measurement of the oscillator. We aim to shed some light on the possibilities to perform qubit QND measurements with such a setup, and to understand whether deviations from the expected behavior could arise from quantum tunneling between the qubit states. Such a tunneling process, although made small compared to the qubit energy splitting, violates the QND conditions.

One of the possible implementations of the system under consideration is the four-junction persistent current

qubit^{14,27,29} (flux qubit) depicted in Fig. 1(a). It consists of a superconducting loop with four Josephson junctions and its low temperature dynamics is confined to the two lowest-energy states. For an external magnetic flux close to a half-integer multiple of $\Phi_0 = h/2e$, the superconducting flux quantum, the two lowest-energy eigenstates are combinations of clockwise and counterclockwise circulating current states. These two states represent the qubit. The measurement appa-

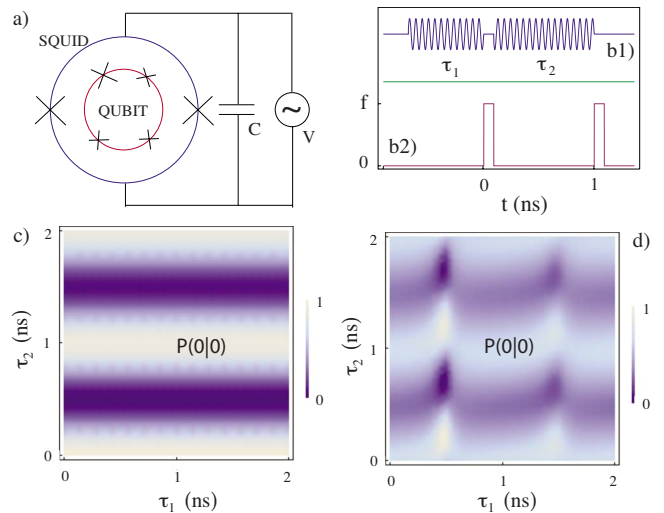


FIG. 1. (Color online) (a) Schematics of the 4-Josephson junction superconducting flux qubit surrounded by a SQUID. (b) Measurement scheme: (b1) two short pulses at frequency $\sqrt{\epsilon^2 + \Delta^2}$, before and between two measurements prepare the qubit in a generic state. Here, ϵ and Δ represent the energy difference and the tunneling amplitude between the two qubit states. (b2) Two pulses of amplitude f and duration $\tau_1 = \tau_2 = 0.1$ ns drive the harmonic oscillator to a qubit-dependent state. (c) Perfect QND: conditional probability $P(0|0)$ for $\Delta = 0$ to detect the qubit in the state 0 vs driving time τ_1 and τ_2 , at Rabi frequency of 1 GHz. The oscillator driving amplitude is chosen to be $f/2\pi = 50$ GHz and the damping rate $\kappa/2\pi = 1$ GHz. (d) Conditional probability $P(0|0)$ for $\Delta/\epsilon = 0.1$, $f/2\pi = 20$ GHz, $\kappa/2\pi = 1.5$ GHz. A phenomenological qubit relaxation time $T_1 = 10$ ns is assumed.

ratus consists of a superconducting quantum interference device (SQUID), composed by two Josephson junctions, inductively coupled to the qubit loop. The SQUID behaves as a nonlinear inductance and, together with a shunt capacitance, forms a nonlinear LC oscillator, which is externally driven. The two qubit states produce opposite magnetic field that translate into a qubit-dependent effective Josephson inductance of the SQUID. The response of the driven SQUID is therefore qubit-dependent.

In order to treat the problem in a fully quantum mechanical way, we linearize the SQUID equation of motion, such that the effective coupling between the driven LC oscillator and the qubit turns out to be quadratic. The qubit Hamiltonian is $\mathcal{H}_S = \epsilon \sigma_Z / 2 + \Delta \sigma_X / 2$. In the experiment,²⁷ the tunneling amplitude Δ between the two qubit current states is made small compared to the qubit gap $E = \sqrt{\epsilon^2 + \Delta^2}$, therefore also $\Delta \ll \epsilon$, such that it can be considered as a small perturbation. The absence of the tunneling term would yield a perfect QND Hamiltonian (see below). From the experimental parameters $\Delta = 5$ GHz and $E = 14.2$ GHz,^{27,30} it follows that $\Delta / \epsilon \approx 0.38$, yielding a reduction in the visibility in Fig. 1(d) on the order of 10%.

The QND character of the qubit measurement is studied by repeating the measurement. A perfect QND setup guarantees identical outcomes for the two repeated measurements with certainty. In order to fully characterize the properties of the measurement, we can initialize the qubit in the state $|0\rangle$, then rotate the qubit by applying a pulse of duration τ_1 before the first measurement and a second pulse of duration τ_2 between the first and the second measurement. The conditional probability to detect the qubit in the states s and s' is expected to be independent of the first pulse, and to show sinusoidal oscillation with amplitude 1 in τ_2 . Deviations from this expectation witness a deviation from a perfect QND measurement. The sequence of qubit pulses and oscillator driving is depicted in Fig. 1(b). The conditional probability $P(0|0)$ to detect the qubit in the state “0” twice in sequence is plotted versus τ_1 and τ_2 in Fig. 1(c) for $\Delta = 0$, and in Fig. 1(d) for $\Delta / \epsilon = 0.1$. We anticipate here that a dependence on τ_1 is visible when the qubit undergoes a flip in the first rotation. Such a dependence is due to the imperfections of the mapping between the qubit state and the oscillator state, and is present also in the case $\Delta = 0$. The effect of the non-QND term $\Delta \sigma_X$ results in an overall reduction of $P(0|0)$.

In this paper, we study the effect of the tunneling term on the quality of a QND measurement. Many attempts to understand the possible origin of the deviations from perfect QND behavior appearing in the experiments have been concerned with the interaction with the environment.^{22,23,30–34} The form of the Josephson nonlinearity dictates the form of the coupling between the qubit and the oscillator, with the qubit coupled to the photon number operator of the driven harmonic oscillator, $\sigma_Z a^\dagger a$, rather than to one quadrature, $\sigma_X(a + a^\dagger)$, and the effect of the tunneling term σ_X present in the qubit Hamiltonian is considered as a small perturbation.

The work we present is not strictly confined to the analysis of superconducting flux qubit measurements. Rather, it is applicable to a generic system of coupled qubit and harmonic oscillator that can find an application in many contexts.

Moreover, the analysis we present is based on the general formalism of the positive operator valued measure (POVM) that represents the most general tool in the study of quantum measurements.

The paper is structured as follows: in Sec. II, we present the idea of QND measurement and describe the conditions under which a QND measurement can be performed. In Sec. III, we derive the quadratic coupling between the qubit and the oscillator and the Hamiltonian of the total coupled system. In Sec. IV, we construct the qubit single measurement with the POVM formalism and in Sec. V we consider the effect of the non-QND term in the POVM that describes the single measurement. In Sec. VI, we construct the two-measurement formalism, by extending the formalism of POVM to the two subsequent measurement case. In Sec. VII, we consider the single measurement in the case $\Delta = 0$ and study the condition for having a good QND measurement. In Sec. VIII, we calculate the contribution at first order and second order in Δ / ϵ to the POVM and to the outcome probability for the qubit single measurement. In Sec. IX, we calculate the contribution at first and second order in Δ / ϵ to the POVM and to the outcome probability for the two subsequent qubit measurements. In Sec. X, we study the QND character of the measurement by looking at the conditional probability for the outcomes of two subsequent measurements when we rotate the qubit before the first measurement and between the first and the second measurement.

II. QND MEASUREMENTS

We consider a quantum system on which we want to measure a suitable observable \hat{A} . A measurement procedure is based on coupling the system under consideration to a meter. The global evolution entangles the meter and the system, and a measurement of an observable \hat{B} of the meter provides information on the system. In general, a strong projective measurement on the meter translates into a weak nonprojective measurement on the system. This is because the eigenstates of the coupled system differ in general from the product of the eigenstates of the measured observable on the system and those of the meter.

Three criteria that a measurement should satisfy in order to be QND have been formulated:^{31,35} (i) correct correlation between the input state and the measurement result; (ii) the action of measuring should not alter the observable being measured; (iii) repeated measurements should give the same result. These three criteria can be cast in a more precise way: *the measured observable \hat{A} must be an integral of motion for the coupled meter and system.*¹ Formally, this means that the observable \hat{A} that we want to measure must commute with the Hamiltonian \mathcal{H} , that describes the interacting system and meter,

$$[\mathcal{H}, \hat{A}] = 0. \quad (1)$$

Such a requirement represents a sufficient condition in order that an eigenstate of the observable \hat{A} , determined by the measurement, does not change under the global evolution of

the coupled system and meter. As a consequence, a subsequent measurement of the same observable \hat{A} provides the same outcome as the previous one with certainty.

Finally, in order to obtain information on the system observable \hat{A} by the measurement of the meter observable \hat{B} , it is necessary that the interaction Hamiltonian does *not* commute with \hat{B} ,

$$[\mathcal{H}_{\text{int}}, \hat{B}] \neq 0, \quad (2)$$

where \mathcal{H}_{int} describes the interaction between the meter and the system,

$$\mathcal{H} = \mathcal{H}_S + \mathcal{H}_{\text{meter}} + \mathcal{H}_{\text{int}}. \quad (3)$$

Altogether, these criteria provide an immediate way to determine whether a given measurement protocol can give rise to a QND measurement. At this level, the observables \hat{A} and \hat{B} and the Hamiltonian \mathcal{H} do not pertain to any particular system. In the next section, we will identify each term for the system we want to study.

III. MODEL: QUADRATIC COUPLING

As far as the application of our model to the measurement of a persistent current qubit with a SQUID is concerned, we provide here a derivation of the quadratic coupling mentioned in the introduction.

We identify the system with a flux qubit that will be described by the Hamiltonian \mathcal{H}_S . The meter is represented by a SQUID and it is inductively coupled to a flux qubit via a mutual inductance, in such a way that the qubit affects the magnetic flux through the loop of the SQUID. The Hamiltonian that describes the SQUID and the interaction with the qubit can be written as

$$\mathcal{H}_{\text{meter}} + \mathcal{H}_{\text{int}} = \frac{\hat{Q}^2}{2C} - \frac{\Phi_0^2}{L_J} \cos(2\pi\hat{\Phi}/\Phi_0) \cos \hat{\varphi}, \quad (4)$$

where $\hat{\varphi} = \hat{\varphi}_1 - \hat{\varphi}_2$ is the difference of the phases of the two Josephson junctions $\hat{\varphi}_1$ and $\hat{\varphi}_2$ that interrupt the SQUID loop, L_J the Josephson inductance of the junctions (nominally equal), and \hat{Q} is the difference of the charges accumulated on the capacitances C that shunt the junctions. Up to a constant factor, $\hat{\varphi}$ and \hat{Q} are canonically conjugate variables that satisfy $[\hat{\varphi}, \hat{Q}] = 2ei$. We split the external flux into a constant term and a qubit-dependent term, such that $\cos(2\pi\hat{\Phi}/\Phi_0) = \cos(2\pi\Phi_{\text{ext}}/\Phi_0 + 2\pi MI_q \sigma_Z / \Phi_0) \equiv \lambda_0 + \lambda_1 \sigma_Z$, with I_q the current in the qubit loop and M the mutual inductance between qubit and SQUID loop. Expanding the potential up to second order in $\hat{\varphi}$, one obtains

$$\mathcal{H}_{\text{meter}} + \mathcal{H}_{\text{int}} \approx \frac{\hat{Q}^2}{2C} + (\lambda_0 + \lambda_1 \sigma_Z) \left(\frac{\Phi_0}{2\pi} \right)^2 \frac{\hat{\varphi}^2}{2L_J}, \quad (5)$$

with $\lambda_0 = \cos(2\pi\Phi_{\text{ext}}/\Phi_0) \cos(2\pi MI_q/\Phi_0)$ and $\lambda_1 = -\sin(2\pi\Phi_{\text{ext}}/\Phi_0) \sin(2\pi MI_q/\Phi_0)$. We introduce the zero point fluctuation amplitude $\sigma = (L_J/\lambda_0 C)^{1/4}$, the bare harmonic oscillator frequency $\omega_{\text{ho}} = \sqrt{\lambda_0/L_J C}$, and the in-phase and in-quadrature components of the field

$$\frac{\Phi_0}{2\pi} \hat{\varphi} \equiv \hat{X} = \sigma \sqrt{\frac{\hbar}{2}} (a + a^\dagger), \quad (6)$$

$$\hat{Q} \equiv \hat{P} = -\frac{i}{\sigma} \sqrt{\frac{\hbar}{2}} (a - a^\dagger), \quad (7)$$

with a and a^\dagger harmonic oscillator annihilation and creation operators satisfying $[a, a^\dagger] = 1$. Apart from a renormalization of the qubit splitting, the Hamiltonian of the coupled qubit and linearized SQUID turns out to be

$$\mathcal{H}_{\text{meter}} + \mathcal{H}_{\text{int}} = \hbar \omega_{\text{ho}} (1 + \tilde{g} \sigma_Z) a^\dagger a + \hbar \omega_{\text{ho}} \tilde{g} \sigma_Z (a^2 + a^{\dagger 2}), \quad (8)$$

with $\tilde{g} = \lambda_1/2\lambda_0 = \tan(2\pi\Phi_{\text{ext}}/\Phi_0) \tan(2\pi MI_q/\Phi_0)/2$. The frequency of the harmonic oscillator describing the linearized SQUID is then effectively split by the qubit.

The Hamiltonian can now be written in the form of Eq. (3) with an additional driving term (from here on we set $\hbar = 1$),

$$\mathcal{H}(t) = \mathcal{H}_S + \mathcal{H}_{\text{meter}} + \mathcal{H}_{\text{int}} + \mathcal{H}_{\text{drive}}(t). \quad (9)$$

The qubit Hamiltonian written by means of the Pauli matrices σ_i (we denote 2×2 matrices in qubit space with bold symbols) in the basis of the current states $\{|0\rangle, |1\rangle\}$ is

$$\mathcal{H}_S = \frac{\epsilon}{2} \sigma_Z + \frac{\Delta}{2} \sigma_X, \quad (10)$$

where $\epsilon = 2I_q(\Phi_{\text{ext}} - \Phi_0/2)$ represents an energy difference between the qubit states and Δ the tunneling term between these states. The Hamiltonian of the oscillator (or SQUID) is

$$\mathcal{H}_{\text{meter}} = \omega_{\text{ho}} a^\dagger a. \quad (11)$$

The Hamiltonian that describes the coupling between the qubit and the harmonic oscillator in the rotating wave approximation (RWA), where we neglected the terms like a^2 and $a^{\dagger 2}$, is given by

$$\mathcal{H}_{\text{int}} = g \sigma_Z a^\dagger a, \quad (12)$$

with $g = \omega_{\text{ho}} \tilde{g}$ (Ref. 36), and the external driving of the harmonic oscillator is described by

$$\mathcal{H}_{\text{drive}}(t) = f(t)(a + a^\dagger). \quad (13)$$

and throughout this work, we choose a harmonic driving force $f(t) = 2f \cos(\omega_d t)$. Neglecting the fast rotating terms $a e^{-i\omega_d t}$ and $a^\dagger e^{i\omega_d t}$, after moving in the frame rotating with frequency ω_d , the Hamiltonian becomes time independent,

$$\mathcal{H} = \mathcal{H}_S + \Delta \omega_Z a^\dagger a + f(a + a^\dagger), \quad (14)$$

with $\Delta \omega_Z = \omega_Z - \omega_d$, and the qubit-dependent frequency given by $\omega_Z = \omega_{\text{ho}}(1 + \tilde{g} \sigma_Z)$.

The qubit observable that we want to measure is $\hat{A} \equiv \sigma_Z$, and, due to the presence of the term $\Delta \sigma_X/2$, it does not represent an integral of the motion for the qubit, $[\mathcal{H}_S, \sigma_Z] \neq 0$. Therefore the measurement is not supposed to be QND, Eq. (1) not being satisfied. However, for $\Delta \ll \epsilon$ the variation in time of σ_Z becomes slow on the time scale determined by

$1/\epsilon$ and one expects small deviations from an ideal QND case. The presence of the non-QND term σ_X in \mathcal{H}_S inhibits an exact solution and a perturbative approach will be carried out in the small parameter $\Delta/\epsilon \ll 1$.

IV. SINGLE MEASUREMENT

The weak measurement of the qubit is constructed as follows. We choose the initial density matrix ($t=0$) of the total coupled system to be the product state $\rho(0) = \rho_0 \otimes |\hat{0}\rangle\langle\hat{0}|$, with the qubit in the unknown initial state ρ_0 and the oscillator in the vacuum state $|\hat{0}\rangle$, and we let the qubit and the oscillator become entangled during the global time-evolution. We then assume that at time t we perform a strong measurement of the flux quadrature $\hat{X} = \sigma(a + a^\dagger)/\sqrt{2}$, by projecting the oscillator on to the state $|x\rangle\langle x|$. Such a state of the oscillator is quite unphysical, it has infinite energy and infinite indeterminacy of the $\hat{P} = (a - a^\dagger)/\sqrt{2}i$ quadrature. More realistically, what would happen in an experiment is that the oscillator is projected on to a small set of quadrature states centered around x . This can be described as a convolution of the projector $|x\rangle\langle x|$ with a distribution characteristic of the measurement apparatus that can be included in the definition of the qubit weak measurement. However, we choose to keep the model simple and to work with an idealized projection.

In the interaction picture, the projection on the state $|x\rangle\langle x|$ corresponds to the choice to measure the quadrature $\hat{X}(t) = \sigma(ae^{-i\omega_{\text{ho}}t} + a^\dagger e^{i\omega_{\text{ho}}t})/\sqrt{2}$,

$$x(t) = \text{Tr}[\hat{X}\rho(t)] = \text{Tr}[\hat{X}(t)\rho_R(t)], \quad (15)$$

$$\rho_R(t) = \mathcal{U}_R(t)\rho(0)\mathcal{U}_R^\dagger(t), \quad (16)$$

where an expression of $\mathcal{U}_R(t)$ and its derivation is given by Eq. (A5) in Appendix A. The operator $\mathcal{U}_R(t)$ describes the time-evolution of ρ in the rotating frame. The probability to detect the outcome x can then be written as

$$\text{Prob}(x, t) = \text{Tr}[\langle x|\rho_R(t)|x\rangle] = \text{Tr}[\langle x|\mathcal{U}_R(t)|\hat{0}\rangle\rho_0\langle\hat{0}|\mathcal{U}_R^\dagger(t)|x\rangle], \quad (17)$$

where the trace is over the qubit space, and $\{|x\rangle\}$ is a basis of eigenstates of $\hat{X}(t)$. We define the operators

$$\mathbf{N}(x, t) = \langle x|\mathcal{U}_R(t)|\hat{0}\rangle, \quad (18)$$

$$\mathbf{F}(x, t) = \mathbf{N}^\dagger(x, t)\mathbf{N}(x, t), \quad (19)$$

acting on the qubit and, using the property of invariance of the trace under cyclic permutation, we write

$$\text{Prob}(x, t) = \text{Tr} \mathbf{F}(x, t)\rho(0). \quad (20)$$

The state of the system after the measurement is $\rho(x, t) \otimes |x\rangle\langle x|$, with the qubit in the state

$$\rho(x, t) = \frac{\mathbf{N}(x, t)\rho(0)\mathbf{N}^\dagger(x, t)}{\text{Prob}(x, t)}. \quad (21)$$

The operators $\mathbf{F}(x, t)$ are positive, trace- and hermiticity-preserving superoperators (i.e., they map density operators

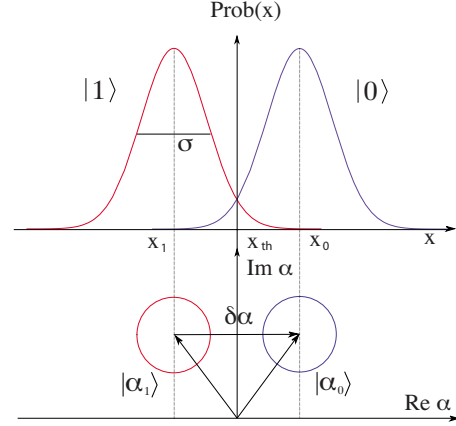


FIG. 2. (Color online) Schematic description of the single-measurement procedure. In the bottom panel the coherent states $|\alpha_0\rangle$ and $|\alpha_1\rangle$, associated with the qubit states $|0\rangle$ and $|1\rangle$, are represented for illustrative purposes by a contour line in the phase space at half-width at half maximum (HWHM) of their Wigner distributions, defined (Ref. 37) as $W(\alpha, \alpha^*) = (2/\pi^2)\exp(2|\alpha|^2)\int d\beta\langle -\beta|\rho|\beta\rangle\exp(\beta\alpha^* - \beta^*\alpha)$. The corresponding Gaussian probability distributions of width σ centered about the qubit-dependent “position” x_s are shown in the top panel.

into density operators) acting on the qubit Hilbert space. Moreover, they satisfy the normalization condition

$$\int_{-\infty}^{\infty} dx \mathbf{F}(x, t) = 1, \quad (22)$$

from which the conservation of probability follows. Therefore, they form a positive operator valued measure (POVM), and we will call the operators $\mathbf{F}(x, t)$ a *continuous* POVM. We point out here that modeling a more realistic scenario, by including a convolution of the projector $|x\rangle\langle x|$ with a distribution characteristic of the measurement apparatus, corresponds to the construction of a more general POVM of the harmonic oscillator that would not alter qualitatively the description of the qubit measurement in terms of POVM.

The probability distribution $\text{Prob}(x, t)$ depends strongly on the initial qubit state ρ_0 . In general $\text{Prob}(x, t)$ is expected to have a two-peak shape, arising from the two possible states of the qubit, whose relative populations determine the relative heights of the two peaks, one peak corresponding to $|0\rangle$ and the other to $|1\rangle$.

We now define an indirect qubit measurement that has two possible outcomes, corresponding to the states “0” and “1.” As a protocol for a single-shot qubit measurement, one can measure the quadrature \hat{X} and assign the state 0 or 1 to the qubit, according to the two possibilities of the outcome x to be greater or smaller than a certain threshold value x_{th} , $x > x_{\text{th}} \rightarrow |0\rangle$, or $x < x_{\text{th}} \rightarrow |1\rangle$, as depicted in Fig. 2. Alternatively, we can infer the qubit state by repeating the procedure many times and constructing the statistical distribution of the outcome x . We then assign the relative populations of the qubit states $|0\rangle$ and $|1\rangle$ by, respectively, integrating the outcome distribution in the regions $\eta(1) = (x_{\text{th}}, \infty)$, $\eta(-1) = (-\infty, x_{\text{th}})$.

We formally condensate the two procedures and define a two-outcome POVM, that describes the two possible qubit outcomes, by writing

$$\mathbf{F}(s,t) = \int_{\eta(s)} dx \mathbf{F}(x,t), \quad (23)$$

$$\text{Prob}(s,t) = \text{Tr}[\mathbf{F}(s,t)\boldsymbol{\rho}(0)], \quad (24)$$

with $s = \pm 1$. We will call $\mathbf{F}(s,t)$ a *discrete* POVM, in contrast to the continuous POVM $\mathbf{F}(x,t)$ defined above. Here, we present a convention that assigns $s=+1$ to the 0 qubit state and $s=-1$ to the 1 qubit state. The probabilities $\text{Prob}(s,t)$ are therefore obtained by integration of $\text{Prob}(x,t)$ on the subsets $\eta(s)$, $\text{Prob}(s,t) = \int_{\eta(s)} dx \text{Prob}(x,t)$. On the other hand, the probability distribution $\text{Prob}(x,t)$ is normalized on the whole space of outcomes, which leads to $P(0,t) + P(1,t) = 1$ at all times. Typically, it is not possible to have a perfect mapping of the qubit state.

V. EFFECTS OF THE TUNNELING σ_X TERM

Deviations from an ideal QND measurement can arise due to the presence of a nonzero σ_X term in the qubit Hamiltonian. In SC flux qubits, such a term is usually present; it represents the amplitude for tunneling through the barrier that separates the two wells of minimum potential, where the lowest-energy qubit current states are located. This term cannot be switched off easily.

We can expand the full evolution operator $\mathcal{U}_R(t)$ in powers of Δt , as in Eq. (A11), and obtain a formally exact expansion of $\mathbf{F}(x,t)$,

$$\mathbf{F}(x,t) = \sum_{n=0}^{\infty} \mathbf{F}^{(n)}(x,t). \quad (25)$$

Due to the transverse ($X \perp Z$) character of the perturbation it follows that the even terms in this series (corresponding to even powers of Δt) have zero off-diagonal entries, whereas the odd terms have zero diagonal entries. Due to the normalization condition Eq. (22), valid at all orders in Δt , it can be shown that

$$\int dx \mathbf{F}^{(n)}(x,t) = \delta_{n,0} \mathbb{1}, \quad (26)$$

and consequently,

$$\sum_{s=\pm 1} \mathbf{F}^{(n)}(s,t) = \delta_{n,0} \mathbb{1}. \quad (27)$$

As a result, the probability $\text{Prob}(s,t)$ is given as a power expansion in the perturbation

$$\text{Prob}(s,t) = \sum_{n=0}^{\infty} \text{Prob}^{(n)}(s,t), \quad (28)$$

where $\sum_{s=\pm 1} \text{Prob}^{(n)}(s,t) = \delta_{n,0}$.

The expansion of the evolution operator and consequently of the continuous and discrete POVMs is in the parameter Δt . The requirement that the deviations introduced by the

tunneling σ_X term in the time-evolution behave as perturbative corrections sets a time scale for the validity of the approximation, namely, $t \ll 1/\Delta$, for which we will truncate the expansion up to second order. The tunneling non-QND term is considered as a perturbation in that experimentally one has $\Delta/\epsilon \ll 1$. It turns out to be convenient to choose as a time scale for the qubit measurement $t \sim 1/\epsilon$, for which follows $\Delta t \sim \Delta/\epsilon \ll 1$.

VI. TWO SUBSEQUENT MEASUREMENTS

A QND measurement implies that repeated measurements give the same result with certainty. In order to verify such a property of the measurement, we construct here the formalism that will allow us to study the correlations between subsequent measurements.

After the oscillator quadrature is measured in the first step at time t and the quadrature value x is detected, the total system composed of the qubit and the oscillator is left in the state $\boldsymbol{\rho}(x,t) \otimes |x\rangle\langle x|$. The fact that we can split the total state after the measurement into a product state is a consequence of the assumption that the measurement of the harmonic oscillator is a projection. Had a more general POVM of the harmonic oscillator be involved, then such a conclusion would not hold. After the first measurement is performed, the total system is left alone under the effects of dissipation affecting the oscillator. A harmonic oscillator that is initially prepared in a coherent state evolves, under weak coupling to a bath of harmonic oscillators in thermal equilibrium, to a mixture of coherent states with a Gaussian distribution centered around the vacuum state (zero amplitude coherent state) with variance $n_{\text{th}} = [\exp(\hbar\omega/k_B T) - 1]^{-1}$, ω being the frequency of the harmonic oscillator, T the temperature, and k_B the Boltzmann constant, whereas in the case $T=0$ it evolves coherently to the vacuum $|\hat{0}\rangle$.³⁷

We now assume that the state of the total system (qubit and oscillator) before the second measurement is

$$\boldsymbol{\rho}(x,t) \otimes |\hat{0}\rangle\langle \hat{0}|. \quad (29)$$

Following the previously described procedure for the qubit single measurement, a second measurement of the quadrature \hat{X} with outcome y performed at time t' , having detected x at time t , would yield the conditional probability distribution

$$\text{Prob}(y,t'|x,t) = \text{Tr}[\mathbf{F}(y,t')\boldsymbol{\rho}(x,t)]. \quad (30)$$

Defining the continuous POVM qubit operators for two measurements as

$$\mathbf{F}(y,t';x,t) = \mathbf{N}^\dagger(x,t)\mathbf{F}(y,t'-t)\mathbf{N}(x,t), \quad (31)$$

the joint probability distributions for two subsequent measurements is

$$\text{Prob}(y,t';x,t) = \text{Prob}(y,t'|x,t)\text{Prob}(x,t) \quad (32)$$

$$= \text{Tr}[\mathbf{F}(y,t';x,t)\boldsymbol{\rho}_0]. \quad (33)$$

The operators $\mathbf{F}(y,t';x,t)$ satisfy the normalization condition $\int dx \int dy \mathbf{F}(y,t';x,t) = \mathbb{1}$, ensuring the normalization of the

probability distribution $\int dx \int dy \text{Prob}(y, t'; x, t) = 1$. By inspection of Eqs. (22) and (31), it follows that

$$\int dy \mathbf{F}(y, t'; x, t) = \mathbf{F}(x, t), \quad (34)$$

and the marginal distribution for the first measurement is

$$\text{Prob}_M(x, t) \equiv \int dy \text{Prob}(y, t'; x, t) = \text{Tr}[\mathbf{F}(x, t)\boldsymbol{\rho}_0], \quad (35)$$

stating that the probability to detect x in the first measurement is independent on whatever could be detected in the second measurement. On the other hand, the marginal probability distribution for the second measurement turns out to be

$$\text{Prob}_M(y, t') \equiv \int dx \text{Prob}(y, t'; x, t) = \text{Tr}[\mathbf{F}(y, t' - t)\boldsymbol{\rho}(t)], \quad (36)$$

where $\boldsymbol{\rho}(t) = \text{Tr}_S[\mathcal{U}_R(t)\boldsymbol{\rho}_0 \otimes |\hat{0}\rangle\langle\hat{0}| \mathcal{U}_R^\dagger(t)]$ is the qubit reduced density matrix at time t . We define the discrete POVM for the correlated outcome measurements as

$$\mathbf{F}(s', t'; s, t) = \int_{\eta(s)} dx \int_{\eta(s')} dy \mathbf{F}(y, t'; x, t). \quad (37)$$

Analogously to Eq. (34), it follows that $\mathbf{F}(s, t) = \sum_{s'} \mathbf{F}(s', t'; s, t)$, and the probability distribution for the outcomes of the two subsequent measurement is simply given by

$$\text{Prob}(s', t'; s, t) = \text{Tr}[\mathbf{F}(s', t'; s, t)\boldsymbol{\rho}_0], \quad (38)$$

and it follows that $\sum_{s'} \text{Prob}(s', t'; s, t) = \text{Prob}(s, t) = \text{Tr}[\mathbf{F}(s, t)\boldsymbol{\rho}_0]$. The conditional probability to obtain a certain outcome s' at time t' , having obtained s at time t , is given by

$$\text{Prob}(s', t' | s, t) = \frac{\text{Tr}[\mathbf{F}(s', t'; s, t)\boldsymbol{\rho}_0]}{\text{Tr}[\mathbf{F}(s, t)\boldsymbol{\rho}_0]}. \quad (39)$$

The discrete POVM for the double measurement can be in general written as

$$\mathbf{F}(s', t'; s, t) \equiv \frac{1}{2}[\mathbf{F}(s', t')\mathbf{F}(s, t) + \text{h.c.}] + \mathbf{C}(s', t'; s, t), \quad (40)$$

where we have symmetrized the product of the two single-measurement discrete POVM operators $\mathbf{F}(s', t')$ and $\mathbf{F}(s, t)$ in order to preserve the hermiticity of each of the two terms of Eq. (40).

Proceeding as for the case of a single qubit measurement, we expand $\mathbf{F}(y, t'; x, t)$ in powers of Δ/ϵ . Equating all the equal powers of Δ/ϵ in the expansion it follows that

$$\mathbf{F}^{(n)}(s, t) = \sum_{s'} \mathbf{F}^{(n)}(s', t'; s, t), \quad (41)$$

with $\sum_{ss'} \mathbf{F}^{(n)}(s', t'; s, t) = \delta_{n,0} \mathbb{1}$.

VII. IDEAL SINGLE MEASUREMENT

The dynamics governed by $\mathcal{U}_R^{(0)}(t)$ produces a coherent state of the oscillator, whose amplitude depends on the qubit state, see Fig. 2. In this case the continuous POVM operators have the simple form $\mathbf{F}^{(0)}(x, t) = \langle \boldsymbol{\alpha}_Z(t) | x \rangle \langle x | \boldsymbol{\alpha}_Z(t) \rangle$, defined through Eq. (A9) in the Appendix A. In the $\boldsymbol{\sigma}_Z$ -diagonal basis $\{|i\rangle\}$, with $i=0, 1$, it is given by

$$\mathbf{F}^{(0)}(x, t)_{ij} = \delta_{ij} \mathcal{G}[x - x_i(t)], \quad (42)$$

where $x_i(t) = \sqrt{2}\sigma \text{Re}[\alpha_i(t)]$ and $\mathcal{G}(x) = \exp(-x^2/\sigma^2)/\sigma\sqrt{\pi}$ is a Gaussian of width σ schematically depicted in Fig. 2. Introducing a rate κ that describes the Markovian damping of the harmonic oscillator by a zero-temperature bath of harmonic oscillators, the coherent state qubit-dependent amplitude $\alpha_i(t)$ is found to be³⁸

$$\alpha_i(t) = A_i e^{i\phi_i} [1 - e^{-i\Delta\omega_i t - \kappa t/2}], \quad (43)$$

with $\Delta\omega_i = \omega_i - \omega_d$ and the qubit-dependent amplitudes and phases given by

$$A_i = \frac{f}{\sqrt{(\Delta\omega_i)^2 + \kappa^2/4}} \quad (44)$$

$$\phi_i = \arctan\left(\frac{\Delta\omega_i}{\kappa/2}\right) - \frac{\pi}{2}. \quad (45)$$

The probability distribution for the \hat{X} quadrature outcomes is then given by the sum of the two qubit-dependent Gaussians, weighted by the initial state occupancy, and the discrete POVM for the qubit measurement as given by Eq. (23) becomes

$$\mathbf{F}^{(0)}(s, t) = \frac{1}{2} \left[1 + s \text{erf}\left(\frac{\delta x(t)}{\sigma}\right) \boldsymbol{\sigma}_Z \right], \quad (46)$$

where $s = \pm 1$ labels the two possible measurement outcomes, and $\delta x(t) = \sigma \text{Re} \delta\alpha(t)/\sqrt{2}$, where $\delta\alpha(t) = \alpha_0(t) - \alpha_1(t)$. The indirect qubit measurement gives the outcome probability

$$\text{Prob}(s, t) = \frac{1}{2} \left[1 + s \text{erf}\left(\frac{\delta x(t)}{\sigma}\right) \langle \boldsymbol{\sigma}_Z \rangle_0 \right], \quad (47)$$

with $\langle \boldsymbol{\sigma}_Z \rangle_0 = \text{Tr}[\boldsymbol{\sigma}_Z \boldsymbol{\rho}_0]$. Supposing that the qubit is prepared in the $|0\rangle$ state, one expects to find $\text{Prob}(0) = 1$ and $\text{Prob}(1) = 0$. From Eq. (47), we see that even for $\Delta = 0$ this is not always the case.

Short time

We choose a time $t \approx 1/\epsilon$ and a driving frequency close to the bare harmonic oscillator frequency. We can then expand the qubit-dependent signal and obtain the short time behavior of the signal difference,

$$\delta\alpha(t) \approx \sqrt{2}tA, \quad (48)$$

with $A = f(e^{2i\phi_0} - e^{2i\phi_1})/\sqrt{2}$. The first nonzero contribution is linear in t , because the signal is due to the time-dependent driving.⁶ We measure a rotated quadrature $\hat{X}_\varphi = \sigma(ae^{-i\varphi}$

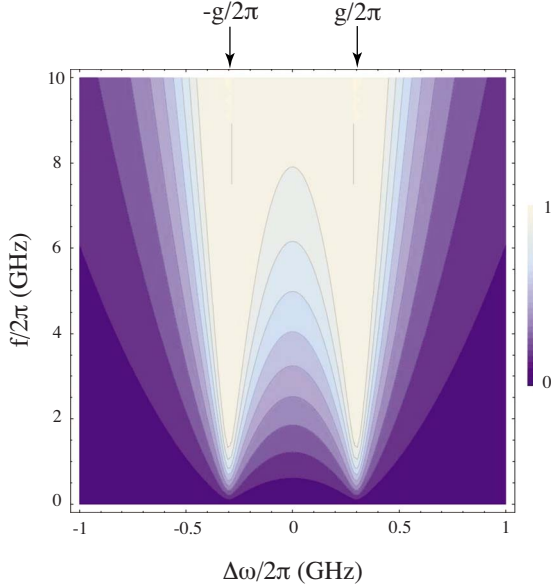


FIG. 3. (Color online) $\text{Prob}(0, t=0.1 \text{ ns})$ for the initial state $|0\rangle\langle 0|$, as given by Eq. (49), plotted as a function of the detuning $\Delta\omega/2\pi$. The values of the parameters used are listed in Table I.

$+a^\dagger e^{i\varphi}/\sqrt{2}$, and choose the phase of the local oscillator such that $\varphi = \arg A$. With this choice we have $\delta x(t) = \sigma|A|t$, and the probabilities for the two-measurement outcomes

$$\text{Prob}(s, t) = \frac{1}{2}[1 + s\langle\sigma_Z\rangle_0 \text{erf}(|A|t)]. \quad (49)$$

In Fig. 3, we plot the probability of measuring the 0 state $\text{Prob}(0, t=0.1 \text{ ns})$ as a function of the detuning $\Delta\omega = \omega_{\text{ho}} - \omega_d$ and the driving amplitude f , given that the initial state is 0, $\rho_0 = |0\rangle\langle 0|$. It is possible to identify a region of values of f and $\Delta\omega$ where $\text{erf}(|A|t) \approx 1$ (Ref. 39). It then follows that

$$\text{Prob}(s) \approx \frac{1}{2}[1 + s\langle\sigma_Z\rangle_0]. \quad (50)$$

This case corresponds to a strong projective measurement, for which the outcome probabilities are either 0 or 1, thus realizing a good qubit single measurement.

For driving at resonance with the bare harmonic oscillator frequency ω_{ho} , the state of the qubit is encoded in the phase of the signal, with $\phi_1 = -\phi_0$, and the amplitude of the signal is actually reduced, as also shown in Fig. 3 for $\Delta\omega = 0$. When matching one of the two frequencies ω_i the qubit state is encoded in the amplitude of the signal, as also clearly shown in Fig. 3 for $\Delta\omega = \pm g$. Driving away from resonance can give rise to significant deviation from 0 and 1 to the outcome probability, therefore resulting in an imprecise mapping between qubit state and measurement outcomes and a weak qubit measurement.

VIII. CORRECTIONS DUE TO TUNNELING

In order to compute the correction at first order in the tunneling term proportional to Δ , we expand the evolution operator $\mathcal{U}_R(t)$ up to first order in Δt . By making use of the

TABLE I. Values of the parameters used in the plots.

Quantity	Symbol	Value for plots
Qubit detuning	ϵ	$2\pi \times 10 \text{ GHz}$
Damping rate	κ	$2\pi \times 0.1 \text{ GHz}$
Coupling strength	g	$2\pi \times 0.3 \text{ GHz}$
Qubit tunneling	Δ/ϵ	0.1

expression Eq. (A12) for the perturbation in the interaction picture, the off-diagonal element of the first order correction to $\mathbf{F}(x, t)$ is given by

$$F^{(1)}(x, t)_{01} = -i \frac{\Delta}{2} \int_0^t dt' \{ \mathcal{G}[x - x_0(t) + \delta z(t')] - \mathcal{G}[x - x_1(t) - \delta z(t')^*] \} e^{i\epsilon t'} \Gamma(t'), \quad (51)$$

with the complex displacement $\delta z(t) = \sigma \delta \alpha(t) / \sqrt{2}$ and the overlap $\Gamma(t) = \langle \alpha_0(t) | \alpha_1(t) \rangle$, where

$$\Gamma(t) = \exp\left(-\frac{1}{2}|\delta \alpha(t)|^2 - i \text{Im}[\alpha_0^*(t) \alpha_1(t)]\right). \quad (52)$$

Here, the state 0 is labeled by its σ_Z eigenvalue $s=1$, whereas the state 1 by its σ_Z -eigenvalue $s=-1$. Analogously to the unperturbed case, the first order contribution to the discrete POVM is obtained by integrating the continuous POVM in x over the subsets $\eta(s)$. Defining the function

$$F^{(1)}(t) = i \frac{\Delta}{2} \int_0^t dt' e^{i\epsilon t'} \Gamma(t') \text{erf}\left(\frac{\delta x(t) - \delta z(t')}{\sigma}\right), \quad (53)$$

we can write the first order contribution to the discrete POVM as

$$\mathbf{F}^{(1)}(s, t) = s(\text{Re } F^{(1)}(t) \sigma_X - \text{Im } F^{(1)}(t) \sigma_Y), \quad (54)$$

and the resulting first order correction to the probability follows directly from Eq. (20). This correction is valid only for short time, $t \ll 1/\Delta$. For times comparable with $1/\Delta$, a perturbative expansion of the time-evolution operator is not valid. Choosing $t \approx 1/\epsilon$, we can effectively approximate the phase associated with two different coherent states as $\text{Im}[\alpha_0(t) \alpha_1(t)^*] \approx \psi t^2$, with $\psi = f^2 \sin(2\phi_0 - 2\phi_1)$, the expression for $F^{(1)}(t)$ further simplifies,

$$F^{(1)}(t) = i \frac{\Delta}{2} \int_0^t dt' e^{i\epsilon t' - 1/2|A|^2 t'^2 - i\psi t'^2} \text{erf}[|A|(t-t')]. \quad (55)$$

We study the behavior of $F^{(1)}(t)$ as a correction to a qubit projective measurement, that is in the range of driving amplitudes and frequencies that ensure $\text{erf}(|A|t) \approx 1$.

The real and imaginary part of $F^{(1)}(t)$ represent the first order correction to the outcome probability of the measurement for two particular initial states, respectively $|+\rangle_X \langle +|$ and $|+\rangle_Y \langle +|$, with $|\pm\rangle_X = (|0\rangle \pm |1\rangle) / \sqrt{2}$ and $|\pm\rangle_Y = (|0\rangle \pm i|1\rangle) / \sqrt{2}$. In the first case we have

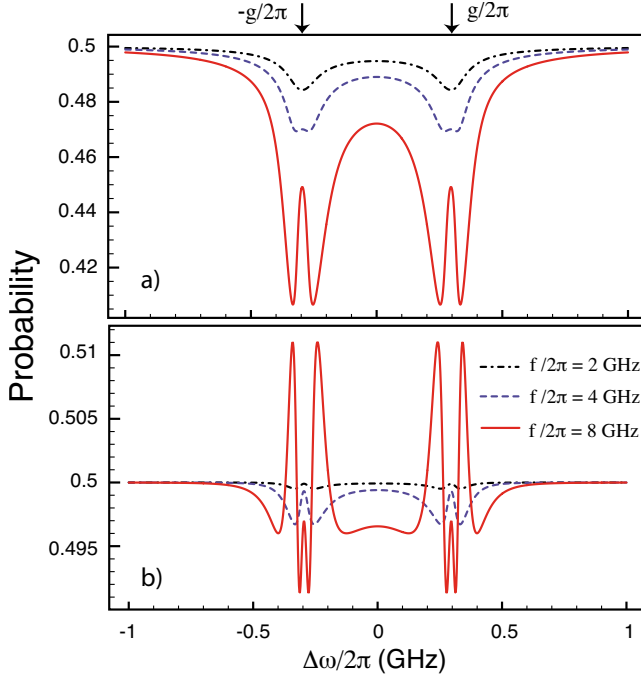


FIG. 4. (Color online) Probability to detect the outcome $s=1$, corrected by (a) the real part of $F^{(1)}$, for the initial state $|+\rangle_X\langle+|$, and (b) the imaginary part of $F^{(1)}$, for the initial state $|+\rangle_Y\langle+|$, plotted vs the detuning $\Delta\omega/2\pi$ for several values of the amplitude f . The values of the parameters used are listed in Table I.

$$\text{Prob}(s,t) = \frac{1}{2} + s \text{Re } F^{(1)}(t), \quad (56)$$

and analogously for the second case, with the imaginary part instead of the real one. We see that the probability to obtain 0 is increased by $\text{Re } F^{(1)}(t)$ and the probability to obtain 1 is decreased by the same amount. Since the contribution to first order in Δt only affects the off-diagonal elements of ρ_0 , there is no effect at first order for the qubit basis states $|0\rangle$ and $|1\rangle$.

In Fig. 4(a), we plot the probability to detect the state 0, corresponding to the outcome $s=1$, corrected up to first order in the perturbation for $\Delta t = \Delta/\epsilon = 0.1$, for the initial state $\rho_0 = |+\rangle_X\langle+|$, that involves $\text{Re } F^{(1)}(t)$. We see that the effect of the tunneling is largest when driving at resonance with the two qubit-shifted frequencies, $\Delta\omega \approx \pm g$. For weak driving amplitude f , the phase ψ in Eq. (55) is small and the response is on order of $\sim 1\%$, close to the qubit-split frequency. By increasing the strength of the driving we see that the structure acquires two local minima in proximity of the resonance $\Delta\omega \approx \pm g$ and a maximum exactly at resonance $\Delta\omega = \pm g$. The strong oscillatory behavior of the probability is due to a rapid change in sign of the phase ψ in proximity of the qubit-split frequencies that is enhanced when the driving strength f increases. In Fig. 4(b), we plot the probability to detect the outcome state 0, corresponding to the outcome $s=1$ for the initial state $\rho_0 = |+\rangle_Y\langle+|$, that involves $\text{Im } F^{(1)}(t)$. In comparison to Fig. 4(a), we find twice as many oscillations in the structure, typical for the imaginary part of a response function, when compared to the real part, and an overall scale factor of order 0.1. Besides, the sign of the response is not

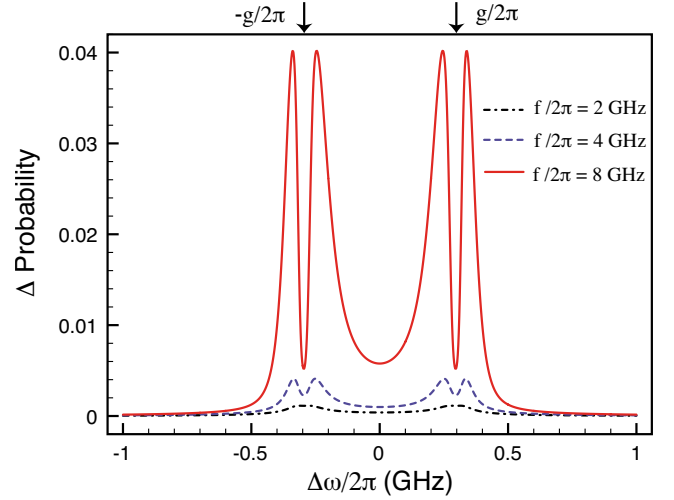


FIG. 5. (Color online) Plot of the second order correction $\text{Prob}^{(2)}(s=1)$ to detect 1 for the initial state $|0\rangle\langle 0|$, for $\Delta t = \Delta/\epsilon$, as a function of the detuning $\Delta\omega/2\pi$, for several values of the driving amplitude f . The values of the parameters for the evaluation used are listed in Table I.

unique. The scale factor and the sign are understood from the Hamiltonian of the qubit, $\mathcal{H} = (\epsilon\sigma_Z + \Delta\sigma_X)/2$, with the condition $\Delta \ll \epsilon$. Under free evolution for a time $t \sim 1/\epsilon$, the initial state $|+\rangle_X\langle+|$ acquires a larger component in the Z-direction than the initial state $|+\rangle_Y\langle+|$. Deviation from this naive picture due to the coupling with the measurement apparatus translates in fluctuations that may determine a change in sign in the response for the case $\rho_0 = |+\rangle_Y\langle+|$. Away from the resonances we see no significant contribution to the outcome probability.

First order effects in the tunneling cannot be responsible for qubit flip during the measurement. In order to estimate the deviation from a perfect QND measurement for the eigenstates of σ_Z , we have to consider the effect of the perturbation at second order. We define $F^{(2)}(t)$ in Eq. (B5) and the contribution at second order in Δt to the discrete POVM is then

$$\mathbf{F}^{(2)}(s,t) = -sF^{(2)}(t)\sigma_Z. \quad (57)$$

The dependence on s factorizes, as expected from the symmetry between the states $|0\rangle$ and $|1\rangle$, in the picture we consider with no relaxation mechanism. The correction at second order in Δ/ϵ to the outcomes probability is given by

$$\text{Prob}^{(2)}(s,t) = -sF^{(2)}(t)\langle\sigma_Z\rangle_0. \quad (58)$$

In Fig. 5, we plot the second order correction to the probability to obtain 1 having prepared the qubit in the initial state $\rho_0 = |0\rangle\langle 0|$, corresponding to $F^{(2)}(t)$, for $\Delta t = \Delta/\epsilon = 0.1$. We choose to plot only the deviation from the unperturbed probability because we want to highlight the contribution to spin-flip purely due to tunneling in the qubit Hamiltonian. In fact most of the contribution to spin-flip arises from the unperturbed probability, as it is clear from Fig. 3. Around the two qubit-shifted frequencies, the probability has a two-peak structure whose characteristics come entirely from the behavior of the phase ψ around the resonances $\Delta\omega \approx \pm g$. We

note that the tunneling term can be responsible for a probability correction up to $\sim 4\%$ around the qubit-shifted frequency.

From the analysis of the qubit single measurement in Fig. 3 we conclude that a weak POVM qubit measurement, that yields a large error in the determination of the qubit state, can arise when weakly driving the harmonic oscillator. Therefore, only a strong qubit projective measurement, obtained for strong driving of the oscillator, can produce a confident mapping of the qubit state at the level of a single measurement. In this case, a deviation on the order of a few percent in the state assignment can be ascribable to the tunneling term.

IX. QND CHARACTER OF THE QUBIT MEASUREMENT

As explained in Sec. II, repeated measurements should give the same result if the measurement is QND. Such a requirement means that if a measurement projects the system onto an eigenstate of the measured observable, then a subsequent measurement should give the same result with certainty. The presence of a term that does not satisfy the QND condition may affect the character of the measurement essentially in two ways: (i) by introducing deviations from the projection character of the single measurement, and (ii) by generating nonzero commutators in the two-measurement POVM. These may affect the two-outcome probabilities.

A. $\Delta=0$ case

The case $\Delta=0$ satisfies the requirement for a QND measurement of the qubit observable σ_Z . The discrete POVM factorizes in this particular case, by virtue of the fact that $[\mathbf{N}^{(0)}(y, t'-t), \mathbf{N}^{(0)}(x, t)]=0$,

$$\mathbf{F}^{(0)}(s', t'; s, t) = \mathbf{F}^{(0)}(s', t' - t) \mathbf{F}^{(0)}(s, t). \quad (59)$$

Choosing, e.g., $t'=2t$ and using Eq. (38), the joint probability for the two measurements reads

$$\begin{aligned} \text{Prob}(s'; s) = & \frac{1}{4} \left[1 + s's \operatorname{erf}\left(\frac{\delta x(t)}{\sigma}\right)^2 \right. \\ & \left. + (s' + s) \operatorname{erf}\left(\frac{\delta x(t)}{\sigma}\right) \langle \sigma_Z \rangle_0 \right]. \quad (60) \end{aligned}$$

In the region of driving frequency and amplitude that ensure $\operatorname{erf}(\delta x/\sigma) \approx 1$, we find

$$\text{Prob}(s'|s) = \frac{1 + s's + (s + s') \langle \sigma_Z \rangle_0}{2(1 + s \langle \sigma_Z \rangle_0)}, \quad (61)$$

with $\text{Prob}(s;s) = \text{Prob}(s)$, and $\text{Prob}(-s;s) = 0$, and the conditional probability is $\text{Prob}(s|s) = 1$, and $\text{Prob}(-s|s) = 0$, regardless of $\langle \sigma_Z \rangle_0$. However, it has to be noticed that in the case the condition $\operatorname{erf}(\delta x/\sigma) \approx 1$ does not perfectly hold, the conditional probability for the two measurements to give the same outcome becomes

$$\text{Prob}(s|s) = \frac{1 + \operatorname{erf}(\delta x/\sigma)^2 + 2s \operatorname{erf}(\delta x/\sigma) \langle \sigma_Z \rangle_0}{2[1 + s \operatorname{erf}(\delta x/\sigma) \langle \sigma_Z \rangle_0]}, \quad (62)$$

and this does depend on the initial state $\langle \sigma_Z \rangle_0$.

B. First order contribution

We now apply the perturbative approach in Δt to estimate the effect of the non-QND term for the joint and the conditional probabilities. Due to the transverse nature of the perturbation, it is possible to show that all the odd terms have off-diagonal entries, whereas even ones are diagonal. At first order in Δt the off-diagonal term of the discrete POVM is given by

$$F^{(1)}(s', t'; s, t) = \frac{s}{2} F^{(1)}(t) + \frac{s'}{2} F^{(1)}(t' - t) + s' C^{(1)}(t'; t), \quad (63)$$

with the quantity $C^{(1)}(t'; t)$ given by Eq. (B6) in Appendix B. For the particular choice $t'=2t$, for which the two measurement procedures are exactly the same, the joint probability for the initial state $\rho_0 = |+\rangle_X \langle +|$ is given at first order in Δt by

$$\begin{aligned} \text{Prob}(s', s) = & \frac{1}{4} \left(1 + s's \operatorname{erf}\left(\frac{\delta x(t)}{\sigma}\right)^2 \right) + \frac{1}{2} (s + s') \operatorname{Re} F^{(1)}(t) \\ & + s' \operatorname{Re} C^{(1)}(2t; t). \quad (64) \end{aligned}$$

We immediately observe that the probability is not symmetric with respect to s and s' . Although the driving times are the same, something is different between the first and the second measurement, and the probability to obtain different outcomes $s' = -s$ is different from zero. An analogous result holds for the initial state $\rho_0 = |+\rangle_Y \langle +|$, with the imaginary part instead of the real one. Now, no matter the sign of $C^{(1)}$, the product $-sC^{(1)}$ is negative in one case ($s = \pm 1$). In order to ensure that probabilities are non-negative one has to choose Δt small enough such that the first order negative correction due to $C^{(1)}$ remains smaller than the unperturbed probability. If Δt is too large, one needs to take higher orders into account, which should then ensure an overall non-negative probability. The behavior of $C^{(1)}$ as a function of the detuning $\Delta\omega$ and the driving amplitude f is very similar to that of $F^{(1)}$, and we choose not to display it. The only main difference arises in the magnitude, for which we have $|C^{(1)}| \ll |F^{(1)}|$. It is clear that the main deviations in the two-measurement probabilities are mainly due to the errors in the first or second measurement.

C. Second order contribution

The contribution to the discrete POVM at second order in Δt can be divided into a term that factorizes the contributions of the first and the second measurements, as well as a term that contains all the nonzero commutators produced in the rearrangement,

$$\begin{aligned} \mathbf{F}^{(2)}(s', t'; s, t) = & \mathbf{F}^{(0)}(s, t) \mathbf{F}^{(2)}(s', t' - t) + \mathbf{F}^{(2)}(s, t) \mathbf{F}^{(0)}(s', t' - t) \\ & + \frac{1}{2} [\mathbf{F}^{(1)}(s, t) \mathbf{F}^{(1)}(s', t' - t) + \text{h.c.}] \\ & + \mathbf{C}^{(2)}(s', t'; s, t). \quad (65) \end{aligned}$$

The full expression of the $\mathbf{C}^{(2)}$ at second order is rather involved. Choosing $t'=2t$ we then obtain

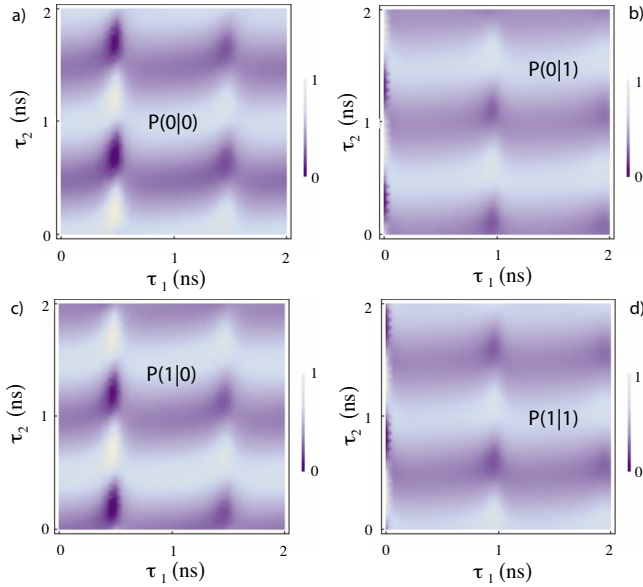


FIG. 6. (Color online) Conditional probability to obtain (a) $s' = s = 1$, (b) $s' = -s = 1$, (c) $s' = -s = -1$, and (d) $s' = s = -1$ for the case $\Delta t = \Delta/\epsilon = 0.1$ and $T_1 = 10$ ns, when rotating the qubit around the y axis before the first measurement for a time τ_1 and between the first and the second measurement for a time τ_2 , starting with the qubit in the state $|0\rangle\langle 0|$. Correction in Δt are up to second order. The harmonic oscillator is driven at resonance with the bare harmonic frequency and a strong driving together with a strong damping of the oscillator are assumed, with $f/2\pi = 20$ GHz and $\kappa/2\pi = 1.5$ GHz.

$$C^{(2)}(p', 2t; p, t)_{ss} = p' p s C^{(2)}(t) - p' p |F^{(1)}(t)|^2, \quad (66)$$

with $C^{(2)}(t)$ given by Eq. (B7) in Appendix B. The probability to obtain identical outcomes does depend on the outcome s itself, and this reflects the fact that the joint probability still depends on the initial states of the qubit. At the same time, the probability for obtaining different outcomes does not depend on s , as expected. However, direct evaluation of the function $C^{(2)}(p', 2t; p, t)$ shows that its contribution to the probability is of order 0.1% and can be neglected.

X. RABI OSCILLATIONS BETWEEN MEASUREMENTS

In order to gain a full insight in the QND character of the measurement, we analyze the behavior of the conditional probability to detect the outcomes s and s' in two subsequent measurements when we perform a rotation of the qubit between the two measurements. Such a procedure has been experimentally adopted in the work of Lupaşcu *et al.*²⁷ When changing the qubit state between the two measurements, only partial QND behavior is expected. In addition to this, we apply an initial rotation to the qubit, such that a wide spectrum of initial states is tested. Ideally, the complete response of this procedure is supposed to be independent on the time τ_1 , during which we rotate the qubit before the first measurement, and to depend only on the time τ_2 , during which we rotate the qubit between the first and the second measurements, with probabilities ranging from zero to one as a function of τ_2 . Such a prediction, once confirmed, would guarantee a full QND character of the measurement.

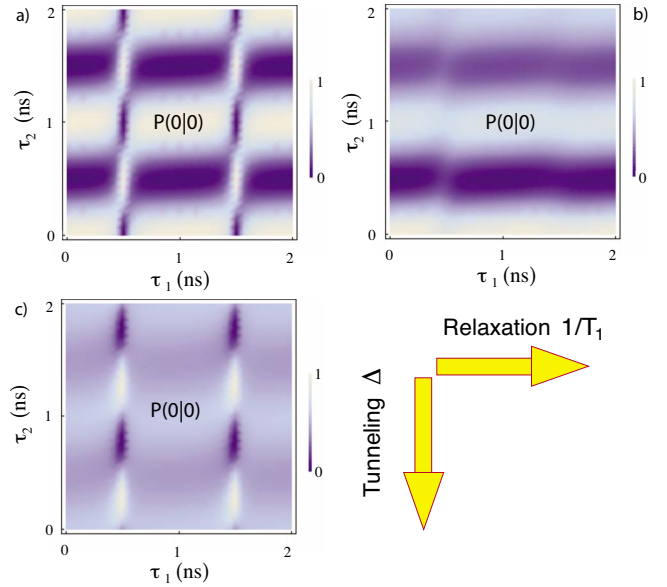


FIG. 7. (Color online) Comparison of the deviations from QND behavior originating from different mechanisms. Conditional probability $P(0|0)$ vs qubit driving time τ_1 and τ_2 starting with the qubit in the state $|0\rangle\langle 0|$, for (a) $\Delta = 0$ and $T_1 = \infty$, (b) $\Delta = 0$ and $T_1 = 2$ ns, and (c) $\Delta = 0.1\epsilon$ and $T_1 = \infty$. The oscillator driving amplitude is $f/2\pi = 20$ GHz and a damping rate $\kappa/2\pi = 1.5$ GHz is assumed.

In Fig. 1(c), we plot the conditional probability $P(0|0)$ for the case $\Delta = 0$, when strongly driving the harmonic oscillator at resonance with the bare harmonic frequency, $\Delta\omega = 0$. The initial qubit state is chosen to be $|0\rangle\langle 0|$. No dependence on τ_1 appears and the outcomes s and s' play a symmetric role. This is, indeed, what we expect from a perfect QND measurement. In Fig. 6, we plot the four combinations of conditional probability $P(s'|s)$ up to second order corrections in $\Delta t = \Delta/\epsilon = 0.1$ and with a phenomenological qubit relaxation time $T_1 = 10$ ns. We choose $\Delta\omega = 0$, that is at resonance with the bare harmonic frequency. The initial qubit state is $|0\rangle\langle 0|$. Three features appear: (i) a global reduction in the visibility of the oscillations, (ii) a strong dependence on τ_1 when the qubit is completely flipped in the first rotation and (iii) an asymmetry under exchange of the outcomes of the first measurement, with an enhanced reduction in the visibility when the first measurement produces a result that is opposite with respect to the initial qubit preparation $|0\rangle\langle 0|$. Furthermore, we find a weak dependence of the visibility on τ_1 .

We now investigate whether it is possible to identify the contributions of different mechanisms that generate deviations from a perfect QND measurement. In Fig. 7, we study separately the effect of qubit relaxation and qubit tunneling on the conditional probability $P(0|0)$. In Fig. 7(a), we set $\Delta = 0$ and $T_1 = \infty$. The main feature appearing is a sudden change in the conditional probability $P \rightarrow 1 - P$ when the qubit is flipped in the first rotation. This is due to imperfection in the mapping between the qubit state and the state of the harmonic oscillator, already at the level of a single measurement. The inclusion of a phenomenological qubit relaxation time $T_1 = 2$ ns, intentionally chosen very short, yields a strong damping of the oscillation along τ_2 and washes out the

response change when the qubit is flipped during the first rotation. This is shown in Fig. 7(b). The manifestation of the non-QND term comes as a global reduction in the visibility of the oscillations, as clearly shown in Fig. 7(c).

At this level it is clearly possible to associate the observed features to different originating mechanisms: (i) qubit tunneling yields an overall reduction in the visibility of the oscillations and an asymmetry under exchange of the outcomes of the first measurement, (ii) qubit relaxation results in damping along τ_2 and weak dependence of the oscillations on τ_1 , and (iii) deviations from projective measurement show up mostly when the qubit is flipped during the first rotation.

The combined effect of the quantum fluctuations of the oscillator, together with the tunneling between the qubit states, is therefore responsible for deviation from a perfect QND behavior, although a major role is played, as expected, by the non-QND tunneling term. Such a conclusion pertains to a model in which the qubit QND measurement is studied in the regime of strong projective qubit measurement and qubit relaxation is taken into account only phenomenologically. We compared the conditional probabilities plotted in Figs. 6 and 7 directly to Fig. 4 in Ref. 27, where the data are corrected by taking into account qubit relaxation, and find good qualitative agreement.

Our findings can also be compared to the experiment,²⁸ in which the QND character of the measurement is addressed by studying a series of two subsequent measurements, but no qubit rotation is performed between the two measurements. The data in Ref. 28 are affected by strong qubit relaxation. However, from the analysis of the joint probabilities of the outcomes of the two measurements provided in Ref. 28, one can extract the conditional probabilities $P(0|0) \sim 83\%$ [when starting with the qubit initially in the ground state and comparable to Fig. 6(a) at $\tau_1 = \tau_2 = 0$], and $P(0|0) \sim 77\%$ [after a π pulse is applied to the qubit initially in the ground state, that is comparable to Fig. 6(a) at $\tau_1 = 0.5$ ns and $\tau_2 = 0$]. In these cases, one would expect a conditional probability of order 1 and a weak dependence on qubit relaxation. A deviation of order $\sim 20\%$ can be understood within the framework of our model as arising from the non-QND term and from a weak qubit measurement. Besides, from the data provided in Ref. 28, one can extract a probability of $\sim 17\%$ to obtain the excited state, when starting with the qubit in the ground state, already at the level of the single measurement. Such a behavior cannot be understood as a result of qubit relaxation and it can be ascribed to deviations from a projective qubit measurement.

XI. CONCLUSION

In this paper, we have analyzed the QND character of a qubit measurement based on coupling to a harmonic oscillator that works as a pointer to the qubit states. The Hamiltonian that describes the interaction between the qubit and the oscillator does not commute with the qubit Hamiltonian. This would in principle inhibit a QND measurement of the qubit. The term in the qubit Hamiltonian that gives rise to the nonzero commutator is small compared with the qubit energy gap, and in the short time qubit dynamics it can be viewed as

a small perturbation. The perturbative analysis carried out for fast measurements leads us to the conclusion that the effect of the non-QND term can manifest itself as a non negligible correction. A perfect QND measurement guarantees perfect correlations in the outcomes of two subsequent measurements, therefore QND character of the measurement is understood in terms of deviations from the expected behavior. Corrections to the outcome probabilities have been calculated up to second order in the perturbing term.

The ground and excited states of the qubit are affected only at second order by the perturbation, but a general measurement protocol should prescind from the state being measured. Therefore, in the spirit of the experiment of Lupaşcu *et al.*,²⁷ we have studied the conditional probability for the outcomes of two subsequent measurements when rotating the qubit before the first measurement and between the first and the second measurement. In the case where the QND condition is perfectly satisfied, that is when the perturbation is switched off, no dependence of the conditional probability on the duration of the first rotation appears and the Rabi oscillations between the two measurement range from zero to one. This behavior shows perfect QND character of the qubit measurement. On the other hand, the main effect of the non-QND term manifests itself as an overall reduction in the visibility of the oscillations and as an asymmetry between the outcomes of the measurements. An additional dependence on the duration of the first qubit rotation may appear if a projective measurement of the qubit is not achieved already in absence of the perturbing non-QND term. Experimentally the measurement is not projective and relaxation processes inhibit a perfect flip of the qubit before the first measurement.

We point out that our analysis is valid only when the non-QND term $\Delta\sigma_x$ can be viewed as a perturbation, that is for short time $\Delta t \ll 1$ and when the qubit dynamics is dominated by the term $\epsilon\sigma_z$, for $\Delta/\epsilon \ll 1$. Our analysis is not valid for the case $\epsilon=0$. In the present study, we have neglected the nonlinear character of the SQUID, which is not relevant to the fundamental issue described here, but plays an important role in some measurement procedures.^{25–28}

A way to improve the QND efficiency would be simply to switch the tunneling off. In the case of superconducting flux qubit, a possibility toward smaller Δ could be to gate the superconducting islands between the junctions of the qubit loop.⁴⁰ As an operational scheme, one could think of working at finite Δ for logical operations and then at $\Delta=0$ for the measurement.

ACKNOWLEDGMENTS

We acknowledge funding from the DFG within SPP 1285 “Spintronics” and from the Swiss SNF via Grant No. PP02-106310.

APPENDIX A: EXACTLY SOLVABLE CASE: $\Delta=0$

In order to determine the evolution governed by the Hamiltonian equation (14), we single out the term \mathcal{H}_0 diag-

onal in the $\{|s, n\rangle\}$ basis, with $|s\rangle$ the eigenstates of σ_Z and $|n\rangle$ the oscillator Fock states,

$$\mathcal{H} = \mathcal{H}_0 + f(a + a^\dagger) + \frac{\Delta}{2} \sigma_X, \quad (\text{A1})$$

with $\mathcal{H}_0 = \epsilon \sigma_Z / 2 + \Delta \omega_Z a^\dagger a$. We then work in the interaction picture with respect to \mathcal{H}_0 . The Heisenberg equation for the density operator reads $\dot{\rho}_I = -i[\mathcal{H}_I, \rho_I]$, with

$$\mathcal{H}_I = \mathcal{H}_I^{(0)} + V_I, \quad (\text{A2})$$

$$\mathcal{H}_I^{(0)} = f(a e^{-i\Delta \omega_Z t} + a^\dagger e^{i\Delta \omega_Z t}), \quad (\text{A3})$$

$$V_I = \frac{\Delta}{2} (e^{i\hat{\Omega}_n t} \sigma_+ + e^{-i\hat{\Omega}_n t} \sigma_-), \quad (\text{A4})$$

where we define $\hat{\Omega}_n = \epsilon + 2ga^\dagger a$, and $\sigma_\pm = (\sigma_X \pm i\sigma_Y)/2$. We will call $\mathcal{U}_I(t)$ the evolution operator generated by \mathcal{H}_I .

The evolution operator is given by $\mathcal{U}(t) = \exp(-i\omega_d t a^\dagger a - i\mathcal{H}_0 t) \mathcal{U}_I(t)$. For the measurement procedure so far defined, we are interested in the evolution operator in the frame rotation at the bare harmonic oscillator frequency. Therefore,

$$\mathcal{U}_R(t) = \exp(-i\epsilon t \sigma_Z / 2 - i\mathcal{H}_{\text{int}} t) \mathcal{U}_I(t). \quad (\text{A5})$$

For the case $\Delta=0$, the model is exactly solvable and $\mathcal{U}_I^{(0)}(t)$ can be computed via a generalization of the Baker-Hausdorff formula,⁴¹

$$\mathcal{U}_I^{(0)}(t) = D[\gamma_Z(t)], \quad (\text{A6})$$

with the qubit-dependent amplitude $\gamma_Z(t) = -if \int_0^t ds e^{i\Delta \omega_Z s}$. The operator $D(\alpha) = \exp(a^\dagger \alpha - \alpha a^*)$ is a displacement operator,³⁷ and it generates a coherent state when applied to the vacuum $|\alpha\rangle \equiv D(\alpha)|0\rangle = e^{-|\alpha|^2/2} \sum_n (\alpha^n / \sqrt{n!}) |n\rangle$. In the frame rotating at the bare harmonic oscillator frequency, the state of the oscillator is a coherent state whose amplitude depends on the qubit state. A general initial state

$$\rho_{\text{tot}}(0) = \sum_{ij=0,1} \rho_{ij} |i\rangle\langle j| \otimes |\hat{0}\rangle\langle \hat{0}|, \quad (\text{A7})$$

where $|\hat{0}\rangle$ is the harmonic oscillator vacuum state, evolves to

$$\rho_R(t) = \sum_{ij=0,1} \rho_{ij} |i\rangle\langle j| \otimes |\alpha_i(t)\rangle\langle \alpha_j(t)|, \quad (\text{A8})$$

where we define the qubit operators $\alpha_Z(t) \equiv \gamma_Z(t) e^{-ig t \sigma_Z}$, and the object

$$|\alpha_Z(t)\rangle \equiv D(\alpha_Z) |\hat{0}\rangle, \quad (\text{A9})$$

that gives a qubit-dependent coherent state of the harmonic oscillator, once the expectation value on a qubit state is taken, $|\alpha_i(t)\rangle = \langle i | \alpha_Z(t) | i \rangle$, for $i=0, 1$.

Perturbation theory in Δ

For nonzero Δ , a formally exact solution can be written as

$$\mathcal{U}_I(t) = \mathcal{U}_I^{(0)}(t) \mathcal{T} \exp\left(-i\Delta \int_0^t dt' \mathcal{V}_I(t')\right), \quad (\text{A10})$$

with $\mathcal{V}_I(t) = \mathcal{U}_I^{(0)\dagger}(t) V_I(t) \mathcal{U}_I^{(0)}(t)$ and \mathcal{T} the time order operator. For a time scale $t \ll 1/\Delta$ we expand the evolution operator in powers of $\Delta t \ll 1$,

$$\begin{aligned} \mathcal{U}_I(t) \approx & \mathcal{U}_I^{(0)}(t) \left(1 - i\Delta t \int_0^1 ds \mathcal{V}_I(st) \right. \\ & \left. - (\Delta t)^2 \int_0^1 ds \int_0^s ds' \mathcal{V}_I(st) \mathcal{V}_I(s't) \right). \end{aligned} \quad (\text{A11})$$

The interaction picture potential can be written as

$$\mathcal{V}_I(t) = \frac{1}{2} [D(t) \sigma^+ + D^\dagger(t) \sigma^-], \quad (\text{A12})$$

with the oscillator operators $D(t)$ defined as

$$D(t) = D^\dagger[\gamma_0(t)] e^{i\hat{\Omega}_n t} D[\gamma_1(t)] \quad (\text{A13})$$

$$\begin{aligned} & = \exp\{i\epsilon t - i \text{Im}[\alpha_0(t) \alpha_1(t)^*]\} \\ & \times D(-\delta\alpha(t) e^{igt}) e^{2ig t a^\dagger a}. \end{aligned} \quad (\text{A14})$$

Here, $\delta\alpha(t) = \alpha_0(t) - \alpha_1(t)$ is the difference between the amplitudes of the coherent states associated with the two possible qubit states.

APPENDIX B: FIRST AND SECOND ORDER QUANTITIES $C^{(1)}$, $F^{(2)}$ AND $C^{(2)}$

For time $t \approx 1/\epsilon$, we expand the evolution operator in Δt and collect the contributions that arise at second power in (Δ/ϵ) . By making use of the expression Eq. (A12) for the perturbation in the interaction picture we can compute the qubit components of the second order contribution to the continuous POVM. We define

$$\begin{aligned} \mathcal{O}_s(t', t'') & = \exp\{is\epsilon(t' - t'') - is\psi[t'^2 - t''^2]\} \\ & \times \langle \delta\alpha(t') e^{igt'} | \delta\alpha(t'') e^{igt''} \rangle, \end{aligned} \quad (\text{B1})$$

and $\langle \alpha | \beta \rangle$ is the overlap between coherent states, and

$$\xi_s^{(2)}(t', t'') = \delta x_s^{(1)}(t')^* + \delta x_s^{(1)}(t''), \quad (\text{B2})$$

$$\zeta_s^{(2)}(t', t'') = -\delta x_s^{(1)}(t') + \delta x_s^{(1)}(t''). \quad (\text{B3})$$

The first term $\xi_s^{(2)}(t', t'')$ represents the complex displacement of the oscillator position due to the perturbation acting one time at $t'' < t'$ (forward in time), and one time at $-t' > -t''$ (backward in time). The second term $\zeta_s^{(2)}(t', t'')$ represents the displacement of the oscillator due to the perturbation acting two times at $t'' < t' < t$. Between the two perturbations the system evolves freely for the time $t'' - t'$ and accumulates a phase that depends on the difference of the effective qubit-dependent frequencies. In the short time approximation $t \approx 1/\epsilon$ such a phase can be neglected. Integrating the position degree of freedom over the subsets $\eta(s')$, we obtain

$$F^{(2)}(s', t)_{ss} = -s' s \frac{\epsilon^2}{4} \int_0^t dt' \int_0^{t'} dt'' \operatorname{Re} \left\{ \mathcal{O}_s(t', t'') \left[\operatorname{erf} \left(\frac{\delta x(t) + \xi_s^{(2)}(t', t'')}{\sigma} \right) + \operatorname{erf} \left(\frac{\delta x(t) + \xi_s^{(2)}(t', t'')}{\sigma} \right) \right] \right\}, \quad (\text{B4})$$

where $\bar{s} = -s$. This expression has meaning only in the short time approximation. By setting $t \approx 1/\epsilon$, the correction $F^{(2)}(t)$ at second order to the discrete POVM is evaluated to be

$$F^{(2)}(t) = \frac{\epsilon^2}{4} \int_0^t dt' \int_0^{t'} dt'' \cos[\epsilon(t' - t'') - \psi(t'^2 - t''^2)] e^{-1/2|A|^2(t' - t'')^2} \{ \operatorname{erf}[|A|(t + t' + t'')] + \operatorname{erf}[|A|(t - t' + t'')] \}. \quad (\text{B5})$$

In an analog way, we calculate the elements of the first and second order contributions to the double measurement operator C . The off-diagonal matrix element of the first order contribution $C^{(1)}$ is

$$C^{(1)}(t'; t) = \frac{1}{2}(\Gamma(t) - 1)F^{(1)}(t' - t) + \frac{i\Delta}{4} \operatorname{erf} \left(\frac{\delta x(t' - t)}{\sigma} \right) \int_0^t dt'' e^{i\epsilon t''} \Gamma(t''), \quad (\text{B6})$$

and the full expression of the diagonal matrix element of the second order contribution $C^{(2)}$ is

$$C^{(2)}(t) = \frac{\epsilon^2}{8} \int_0^t dt' \int_0^{t'} dt'' e^{i[\epsilon(t' - t'') - \psi(t'^2 - t''^2)]} e^{-|A|^2/2(t' - t'')^2} \operatorname{erf}[|A|(t + t' + t'')] - \operatorname{Im} \left\{ F^{(1)}(t) \epsilon \int_0^t dt' e^{-i\epsilon t'} \Gamma(t) \Gamma(t')^* e^{-1/2|A|^2 t'^2 + |A|^2 t'} \operatorname{erf}[\delta x_{-}^{(1)}(t')/\sigma] \right\}. \quad (\text{B7})$$

*luca.chirolli@uni-konstanz.de

†guido.burkard@uni-konstanz.de

¹V. B. Braginsky and F. Ya. Khalili, *Quantum Measurement* (Cambridge University Press, Cambridge, England, 1992).

²G. J. Milburn and D. F. Walls, *Phys. Rev. A* **28**, 2065 (1983).

³N. Imoto, H. A. Haus, and Y. Yamamoto, *Phys. Rev. A* **32**, 2287 (1985).

⁴H.-A. Bachor, M. D. Levenson, D. F. Walls, S. H. Perlmuter, and R. M. Shelby, *Phys. Rev. A* **38**, 180 (1988).

⁵M. Fortunato, P. Tombesi, and W. P. Schleich, *Phys. Rev. A* **59**, 718 (1999).

⁶A. A. Clerk, S. M. Girvin, and A. D. Stone, *Phys. Rev. B* **67**, 165324 (2003).

⁷D. H. Santamore, A. C. Doherty, and M. C. Cross, *Phys. Rev. B* **70**, 144301 (2004).

⁸I. Dotsenko, M. Mirrahimi, M. Brune, S. Haroche, J.-M. Raimond, and P. Rouchon, *Phys. Rev. A* **80**, 013805 (2009).

⁹E. K. Irish and K. Schwab, *Phys. Rev. B* **68**, 155311 (2003).

¹⁰M. A. Nielsen and I. L. Chuang, *Quantum Computation and Quantum Information* (Cambridge University Press, Cambridge, England, 2000).

¹¹E. Il'ichev, N. Oukhanski, A. Izmalkov, Th. Wagner, M. Grajcar, H.-G. Meyer, A. Yu. Smirnov, A. Maassen van den Brink, M. H. S. Amin, and A. M. Zagoskin, *Phys. Rev. Lett.* **91**, 097906 (2003).

¹²I. Chiorescu, P. Bertet, K. Semba, Y. Nakamura, C. J. P. M. Harmans, and J. E. Mooij, *Nature (London)* **431**, 159 (2004).

¹³M. Grajcar, A. Izmalkov, E. Il'ichev, Th. Wagner, N. Oukhanski, U. Hübner, T. May, I. Zhilyaev, H. E. Hoening, Ya. S. Greenberg, V. I. Shnyrkov, D. Born, W. Krech, H.-G. Meyer, A. Maassen van den Brink, and M. H. S. Amin, *Phys. Rev. B* **69**, 060501(R) (2004).

¹⁴P. Bertet, I. Chiorescu, G. Burkard, K. Semba, C. J. P. M. Harmans, D. P. DiVincenzo, and J. E. Mooij, *Phys. Rev. Lett.* **95**, 257002 (2005).

¹⁵M. A. Sillanpää, T. Lehtinen, A. Paila, Yu. Makhlin, L. Roschier, and P. J. Hakonen, *Phys. Rev. Lett.* **95**, 206806 (2005).

¹⁶T. Duty, G. Johansson, K. Bladh, D. Gunnarsson, C. Wilson, and P. Delsing, *Phys. Rev. Lett.* **95**, 206807 (2005).

¹⁷N. Katz, M. Ansmann, R. C. Bialczak, E. Lucero, R. McDermott, M. Neeley, M. Steffen, E. M. Weig, A. N. Cleland, J. M. Martinis, and A. N. Korotkov, *Science* **312**, 1498 (2006).

¹⁸A. Wallraff, D. I. Schuster, A. Blais, L. Frunzio, R.-S. Huang, J. Majer, S. Kumar, S. M. Girvin, and R. J. Schoelkopf, *Nature (London)* **431**, 162 (2004).

¹⁹A. Blais, R.-S. Huang, A. Wallraff, S. M. Girvin, and R. J. Schoelkopf, *Phys. Rev. A* **69**, 062320 (2004).

²⁰D. I. Schuster, A. Wallraff, A. Blais, L. Frunzio, R.-S. Huang, J. Majer, S. M. Girvin, and R. J. Schoelkopf, *Phys. Rev. Lett.* **94**, 123602 (2005).

²¹A. Wallraff, D. I. Schuster, A. Blais, L. Frunzio, J. Majer, M. H. Devoret, S. M. Girvin, and R. J. Schoelkopf, *Phys. Rev. Lett.* **95**, 060501 (2005).

²²J. Gambetta, A. Blais, D. I. Schuster, A. Wallraff, L. Frunzio, J. Majer, M. H. Devoret, S. M. Girvin, and R. J. Schoelkopf, *Phys. Rev. A* **74**, 042318 (2006).

²³J. Gambetta, W. A. Braff, A. Wallraff, S. M. Girvin, and R. J. Schoelkopf, *Phys. Rev. A* **76**, 012325 (2007).

²⁴M. Boissonneault, J. M. Gambetta, and A. Blais, *Phys. Rev. A* **79**, 013819 (2009).

²⁵I. Siddiqi, R. Vijay, F. Pierre, C. M. Wilson, M. Metcalfe, C. Rigetti, L. Frunzio, and M. H. Devoret, *Phys. Rev. Lett.* **93**, 207002 (2004).

²⁶I. Siddiqi, R. Vijay, M. Metcalfe, E. Boaknin, L. Frunzio, R. J.

- Schoelkopf, and M. H. Devoret, Phys. Rev. B **73**, 054510 (2006).
- ²⁷A. Lupaşcu, S. Saito, T. Picot, P. C. De Groot, C. J. P. M. Harmans, and J. E. Mooij, Nat. Phys. **3**, 119 (2007).
- ²⁸N. Boulant, G. Ithier, P. Meeson, F. Nguyen, D. Vion, D. Esteve, I. Siddiqi, R. Vijay, C. Rigetti, F. Pierre, and M. Devoret, Phys. Rev. B **76**, 014525 (2007).
- ²⁹F. Yoshihara, K. Harrabi, A. O. Niskanen, Y. Nakamura, and J. S. Tsai, Phys. Rev. Lett. **97**, 167001 (2006).
- ³⁰T. Picot, A. Lupascu, S. Saito, C. Harmans, and J. Mooij, Phys. Rev. B **78**, 132508 (2008).
- ³¹T. C. Ralph, S. D. Bartlett, J. L. O'Brien, G. J. Pryde, and H. M. Wiseman, Phys. Rev. A **73**, 012113 (2006).
- ³²I. Serban, E. Solano, and F. K. Wilhelm, Phys. Rev. B **76**, 104510 (2007).
- ³³I. Serban and F. K. Wilhelm, Phys. Rev. Lett. **99**, 137001 (2007).
- ³⁴I. Serban, B. L. T. Plourde, and F. K. Wilhelm, Phys. Rev. B **78**, 054507 (2008).
- ³⁵B. Travaglione, G. Milburn, and T. Ralph, arXiv:quant-ph/0203130 (unpublished).
- ³⁶Experimental data report a qubit-induced differential shift in the bare SQUID frequency about the 4%, yielding $g=0.02$.
- ³⁷M. O. Scully and M. S. Zubairy, *Quantum Optics* (Cambridge University Press, Cambridge, England, 2001).
- ³⁸The factor $1/2$ multiplying the damping rate κ is typical of coherent states arising from driving of a quantum harmonic oscillator, subjected to Markovian damping due to weak coupling to a bath of harmonic oscillator. The damping rate κ can be related to the quality factor Q , $\kappa=\omega_{\text{ho}}/2\pi Q$ (Ref. 37).
- ³⁹Strictly speaking, $\text{erf}(x)$ approaches 1 only asymptotically, in the limit $x\rightarrow\infty$. However, for values of x such that $1-\text{erf}(x)<10^{-4}$, we discard the small deviation from 1.
- ⁴⁰L. Chirolli and G. Burkard, Phys. Rev. B **74**, 174510 (2006).
- ⁴¹C. W. Gardiner and P. Zoller, *Quantum Noise*, 2nd ed. (Springer-Verlag, Berlin, 2000).